

Impact of Surrounding Objects on Inductive Wireless Power Transfer

Master's Thesis

By

Brenda Awuor Odhiambo

Department of Electrical and Information Technology
Faculty of Engineering, LTH, Lund University
SE-221 00 Lund, Sweden



LUND UNIVERSITY



2019

Abstract

Many new models of smartphones and small electronic devices are using their wireless charging feature as a key selling point. This is due to the convenience of cable-free charging as well as not requiring multiple power adapters for charging different devices. However, with the increasing use of devices having wireless charging capability, safety and efficiency issues arise. Safety concerns are critical for manufacturers of these devices. In inductive wireless charging systems, knowledge on the impact of surrounding objects on the system is imperative in designing safer and more efficient systems. This thesis gives a quantitative analysis of the influence of foreign objects to an inductively coupled Wireless Power Transfer (WPT) system. This is done by measuring carefully chosen square metal plates of different dimensions and material properties, and quantifying their impact on the coil inductance, equivalent coil resistance and quality factor of the transmitter coil. Low-frequency electromagnetic simulations are performed in Ansys Maxwell to verify the experimental measurements. The results obtained by experiments and simulations are consistent with each other. These results are analyzed, and conclusions drawn pertaining to how the materials impact the system.

In particular, the tested metal plates increase the equivalent coil resistance as compared to that of the empty coil, due to the induced eddy currents on the plates. Simultaneously, eddy currents tend to decrease the coil inductance as compared to that of the empty coil. However, at frequencies lower than 100 kHz, the presence of ferromagnetic metal plates can actually increase the coil inductance, as these plates are strongly magnetized by the magnetic field generated by the coil currents. In general, the quality factor is decreased in the presence of the test metals. Further, the thickness of the metals influences the power loss due to eddy currents only if the metal thickness is below the skin depth of the metal. In addition, the square metal plates with side lengths equal to or greater than the coil diameter have similar impact on the coil parameters, indicating highly localized magnetic fields around the coil. The metal plates with side lengths smaller than the coil diameter have more unpredictable impacts on coil parameters. Investigations into the impact of foreign objects on both the transmitter and receiver coils are proposed for future work.

Acknowledgments

I would like to extend my heartfelt gratitude to nok9 AB for giving me the opportunity to do this master thesis. Special thanks to my supervisors Buon Kiong Lau and Max Andersson for the invaluable advice, reviews, suggestions and guidance during the entire work. A big thank you to Laurens Swaans for the critical reviews, pertinent questions and input to refine the research. Thank you to all my colleagues at nok9 AB, especially Arianna Amaya, Love Rosén, and Jonatan Nyström for your insights at various stages of the project and Tomas Avramovic for sourcing the materials required.

To my family, I would not be who I am without your love and support.

Contents

Abstract	2
Acknowledgments	3
List of figures	6
List of tables	8
List of acronyms	9
Popular Science Summary	10
1. Introduction.....	11
1.1. Background.....	11
1.2. Justification.....	12
1.3. Objective	13
1.4. Structure.....	13
2. Theoretical Framework	15
2.1. Inductive WPT System.....	15
2.2. Coil Inductance	17
2.3. Equivalent Model of the Coil.....	18
2.4. Q factor.....	19
2.5. Eddy currents	19
2.5.1. Power Loss.....	20
2.6. Magnetic properties of materials.....	20
2.6.1. Permeability	21
3. Methodology	23
3.1. Choice of Samples	23
3.1.1. Parameters of Interest	23
3.1.2. Metal Plate Size	25
3.2. Measurements	26

3.2.1.	Experiment Setup	26
3.2.2.	Variables	27
3.3.	Simulation.....	30
3.3.1.	Simulation Model	30
3.3.2.	Eddy Current Simulations	32
4.	Results and Analysis	37
4.1.	Experimental Measurements	37
4.1.1.	General Impact on Coil Parameters	37
4.1.2.	Impact of Different Sizes of Metal Plates	43
4.1.3.	Impact of Different Thicknesses of Metal Plates.....	45
4.1.4.	Impact of Different Positions of Metal Plates	46
4.2.	Ansys Simulations.....	48
4.2.1.	Impact of Different Positions of Metal Plates	48
4.2.2.	Impact of Different Sizes of Aluminum Plates.....	52
5.	Conclusions and Future Work	55
5.1.	Conclusions.....	55
5.2.	Future Work	56
	References.....	57

List of figures

Figure 2-1: Generic Inductive WPT system	15
Figure 2-2: Transmitter Coil	16
Figure 2-3: Electromagnetic induction in the coil.....	18
Figure 2-4: Coil Equivalent Model	18
Figure 3-1: Coil with inner and outer diameter	25
Figure 3-2: Metal plate sizes used in the study.....	26
Figure 3-3: Experimental setup with the LCR meter, the coil with the square metal plate on top, and a PC for acquiring the measured data.....	27
Figure 3-4: Metal position 1	28
Figure 3-5: Metal position 2	29
Figure 3-6: Metal position 3	29
Figure 3-7: Metal position 4	30
Figure 3-8: Ansys Maxwell model of the transmitter coil (backed by a ferrite plate) without a metal plate.....	32
Figure 3-9: Coil with $15 \times 15 \text{ cm}^2$ stainless steel.....	33
Figure 3-10: Coil with different positions of $2 \times 2 \text{ cm}^2$ stainless steel above	34
Figure 3-11: Coil with $4.3 \times 4.3 \text{ cm}^2$ aluminum above	35
Figure 4-1: Coil inductance change with ferromagnetic metals.....	38
Figure 4-2: Coil inductance change with non-ferromagnetic metals.....	39
Figure 4-3: Equivalent coil resistance with ferromagnetic metals	40
Figure 4-4: Equivalent coil resistance with non-ferromagnetic metals.....	41
Figure 4-5: Observed Q factor with ferromagnetic metals.....	42

Figure 4-6: Observed Q factor with non-ferromagnetic metals.....	43
Figure 4-7: Size $15 \times 15 \text{ cm}^2$ and $4.3 \times 4.3 \text{ cm}^2$ plates on coil inductance	44
Figure 4-8: Size $15 \times 15 \text{ cm}^2$ and $4.3 \times 4.3 \text{ cm}^2$ plates on equivalent coil resistance	44
Figure 4-9: Iron plate of different thicknesses	45
Figure 4-10: Coil inductance for different positions of metal plate	46
Figure 4-11: Equivalent coil resistance for different positions of metal plate	47
Figure 4-12 Ansys simulation effect on equivalent coil resistance with $2.2 \times 2.2 \text{ cm}^2$ stainless steel plate in positions 1 and 2.....	48
Figure 4-13: Current distribution for metal in position 1.....	49
Figure 4-14: Current distribution for metal in position 2.....	50
Figure 4-15: Current distribution for metal in position 3.....	50
Figure 4-16: Current distribution for metal in position 4.....	51
Figure 4-17: Ansys simulation of aluminum metal in different sizes effect on coil inductance.....	52
Figure 4-18: Ansys simulation of aluminum metal in different sizes effect on coil equivalent resistance	53

List of tables

Table 2-1: Coil Parameters.....16

Table 3-1: Material Properties.....24

List of acronyms

DC	Direct Current
FO	Foreign Object
FOD	Foreign Object Detection
IoT	Internet of Things
RMS	Root Mean Square
WPT	Wireless Power Transfer
WPC	Wireless Power Consortium

Popular Science Summary

The global wireless charging market is expected to hit USD\$71 billion by 2025 [1]. With the onset of Internet of Things (IoT) where many hundreds of millions more devices will be connected to the internet, opportunities for wireless charging applications will be further enhanced. Wireless charging of smartphones and wearable electronics is just one of many areas where modern day wireless charging is applied. In general, wireless charging solutions have been applied in consumer electronics, automotive industry and health care. Efforts are also made to promote the same technology for wirelessly powered kitchen appliances.

When wirelessly charging or powering a device, it is desirable to have maximum power transfer efficiency and guaranteed safety of the user. Reduction in the power transferred is mostly caused by surrounding objects that interfere with the wireless charging system [2]. The most obvious safety risk is overheating of the device, which can cause fires. Moreover, even if there is no safety risk, inefficient power transfer results in longer charging times. Therefore, it is important to understand how surrounding objects affect the wireless charging system, so that guidelines can be made to improve system design and appropriate measures taken when foreign objects disturb the system unexpectedly. Examples of foreign objects include coins, keys and safety pins, everyday metallic objects that may be placed near wireless charging pads as wireless devices are being charged.

Currently, the Qi Specification is the dominant wireless charging standard, and it includes safety mechanisms for identifying foreign objects and shutting down the charging process when they are detected. However, given the relatively recent adoption of the wireless charging technology, very little study has been performed on the behavior of wireless charging system when it is subjected to foreign objects. To address this knowledge gap, this thesis investigates the impact of surrounding objects on the metal coil used in the charging pad. Specifically, the surrounding objects are metal plates of different sizes and material properties, and the impact is quantified in terms of several coil parameters, including resistance and inductance. The metals chosen in this study are commonly used ones, including copper, aluminum and stainless steel. The results from the thesis yield practical insights and rule-of-thumbs that can be used for wireless charging system design. For example, metals with ferromagnetic properties tend to have less impact on coil inductance. The knowledge gained can also be used to improve the detection of foreign objects, which will further increase the safety of wireless charging applications.

Chapter

1. Introduction

1.1. Background

Wireless Power Transfer (WPT) system is becoming a popular research area due to its numerous applications [3], [4]. From electric toothbrush, cordless kitchen appliances, to wirelessly charged electric vehicles, researchers and industry giants alike are on the pursuit of making wireless charging even more ubiquitous. Some benefits of having devices being charged wirelessly include convenience, increased device mechanical durability and improved device water-tightness (no need for connector). Thanks to its many benefits over wired charging, this technology is progressively becoming preferable to many consumers[1]. This is especially so for near field WPT systems used in electronic devices, which are experiencing major commercial success. This is evidenced by the Qi standard/specification (based on inductively coupled WPT) attracting household names like Apple, Samsung and Volvo Cars to provide WPT solutions in their products. Today, the Qi standard is by far the most popular standard for near field WPT technology, and it is adopted in hundreds of millions of devices. The Qi standard is developed by the Wireless Power Consortium (WPC), which is a collaborative standards development group with over 600 members all over the world to promote efficient and safe operation, as well as worldwide interoperability, of all wireless chargers and wireless power sources [5].

Wireless charging however is not a new technology, many scientists have performed research on wireless transmission of power for over a century, with very notable contributions by the inventor and scholar Nikola Tesla. Tesla saw a world where WPT would be possible all around the world[6]. Nevertheless, it was not until a hundred years later that the technology was being explored seriously for commercialization. In his early experiments on WPT, Tesla transmitted power wirelessly based on electromagnetic radiation [6]. These were the foundations of WPT and in 1964, William C. Brown developed the rectenna, a practical realization of wireless charging. He demonstrated microwave WPT by charging a helicopter [7]. These methods of power transmission using microwave energy over long distances constitute the far field WPT methods and are mostly used for military or industrial applications [8]. However, it is not feasible to have consumer devices being powered by microwave systems due to safety concerns, technical complexity, efficiency issues and the costs associated with deploying such systems.

Therefore, near field WPT methods are used in these cases, and also due to the required transmission distance being short.

Near field WPT employs electromagnetic induction where power is transferred through magnetic fields. In an inductively coupled WPT system, the transmission distance must remain small for the coupling to hold. Today, the most prevalent use case for inductive WPT is the charging of handheld devices such as mobile phones, tablets and laptops[1]. Even though the basic principles behind inductive coupling are well understood and can be explained using Faraday's law of electromagnetic induction, many research questions remain concerning the design and optimization of inductively coupled WPT systems, especially in relation to different application contexts.

1.2. Justification

It is known that surrounding objects can have significant influence on inductive coupling WPT systems [9]. Specifically, the impact of different materials on WPT coils is not well understood in the wireless charging community. These materials can interact with the magnetic field generated by the coil, which can in turn either distort the incident field or generate an induced field, both of which changes the coil parameters. In general, a foreign object (FO) between the transmitter and receiver of an inductive WPT system degrades the performance of the system. The presence of FOs result can greatly deteriorate efficiency in power transmission and cause heating problems. Several works have been undertaken on Foreign Object Detection (FOD) such as [10] that gives an FOD method for megahertz-range WPT systems and [11] that validates the Power Loss Detection method. The two works focus only on how to detect FOs. In [12], two-port parameter changes are computed to predict the data used to control a WPT system. However, the method is hard to implement due to complicated calculations. An investigation of the effects of foreign metal objects on class-E inverter is given in [13]. The study focuses on the switching conditions of the inverter. Moreover, [13] investigates just two metals.

In all these previous works, there is consideration only for thermal heating from FOs and/or a decline in transfer efficiency. There is little discussion on the actual impact from the surrounding objects on inductive WPT coil parameters. As more and more applications of WPT systems are being implemented, it is important to understand the impact of surrounding objects. In addition, safety of the users is an even more important issue than before. This is leading to the development of new safety regulations and systems robust enough to cater for ever-changing use cases. It is therefore necessary to have knowledge of how surrounding objects may affect an inductive WPT

system. This thesis focuses on quantifying the effect of FOs and further give a prediction of how WPT coil parameters will be affected in the presence of FOs.

1.3. Objective

In this thesis, the primary aim is to quantify and predict the change in the coil inductance, equivalent coil resistance and quality factor of the transmitter coil in inductive WPT due to the presence of surrounding objects. The scope is limited to square plates of different sizes and thicknesses, which are made of different types of metal.

To this end, the focus of the project is to:

- Identify and source a large collection of square metal plates relevant to an inductively coupled WPT system.
- Measure the inductance and resistive loss for the coil subject to the presence of different metal plates.
- Model and validate in electromagnetic simulation the behavior of a selected number of test cases.
- Translate the above knowledge into guidelines and rules-of-thumb for designing inductive coupling WPT system

1.4. Structure

This report is divided into 5 chapters which includes this introductory one. A theoretical framework is given in the following chapter explaining the basic concepts behind some of the parameters investigated in the thesis. Chapter 3 gives the experimental set up and methods used to carry out measurements. Additionally, factors that were considered in making a choice of the samples to use systematically through the research are stated. In Chapter 4, results obtained from experimentation and simulation methods are outlined. Lastly, conclusions are drawn in Chapter 5. A discussion on future work is also presented in this chapter.

Chapter

2. Theoretical Framework

This chapter gives the theoretical background of the main concepts used in this thesis. It begins with a brief overview of an inductive WPT system. The focus is then given to the transmitter coil, and the coil parameters. Further, the concepts of eddy currents and magnetization are introduced, to help readers understand the basis for the choice of samples in the thesis work.

2.1. Inductive WPT System

The basic structure of an inductive WPT is given in Figure 2-1. A real inductively coupled WPT system is a complex structure. The figure is a simplified block diagram version for explaining its basic operation. Complex circuit components of the inverter and rectifier are excluded. The system consists of two parts, a transmit side and a receive side. Alternating current is passed through the transmitter coil and by Ampere's law varying magnetic fields are generated [14]. These magnetic fields are picked up by the receiver coil and a voltage is induced through Faraday's law of electromagnetic induction. By Lenz law, the polarity of the induced voltage is such that the associated current generated results in a magnetic field that opposes the change of magnetic field which produces the induced voltage.

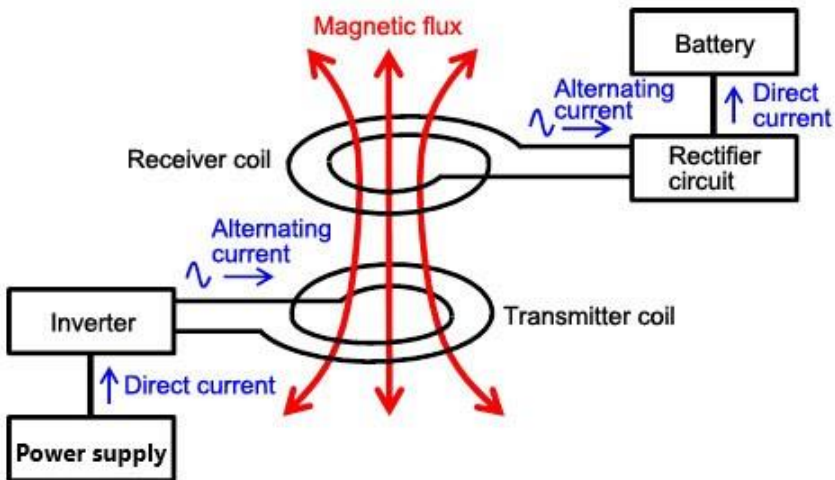


Figure 2-1: Generic Inductive WPT system [15]

In this thesis, only the transmitter coil part of the inductive WPT system was investigated. Power transfer begins from the power source through the transmitter coil. The transmitter coil can employ various methods to discover and locate objects on its surface while not waking up the receiver or starting digital communications. These methods, also known as ‘analog pings’ can be based on resonance shift or capacitance change [16]. If a foreign object is detected, the power transfer process will not be initiated. One transmitter coil is shown in Figure 2-2 and the parameters of the coil are given in Table 2-1. The complete coil consists of two layers of spiral coils, with ten turns each and located on top of a black ferrite plate. This particular coil is used as a power transmitter coil in a Qi standard compliant power transmitter for currents of up to 5 A root mean square (RMS) [17].

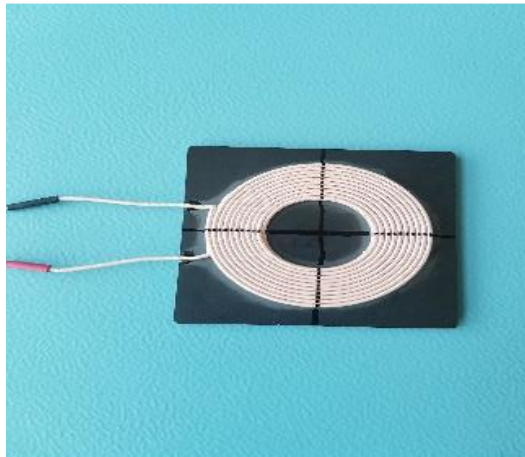


Figure 2-2: Transmitter Coil

Table 2-1: Coil Parameters

Parameter	Value
Coil inner diameter	20.5 mm
Coil outer diameter	43.0 mm
Ferrite width	53.3 mm
Ferrite length	53.3 mm
Ferrite thickness	2.5 mm

2.2. Coil Inductance

Inductance is a property of the coil to oppose the change in the current flowing through it. The opposition to changing current is achieved by having a voltage induced in the coil with a counter polarity to the voltage causing the change in current. Since this induced voltage occurs in the same circuit as that in which the current is changing, then this inductance is known as the self-inductance of the coil. From Ampere's law, when current flowing through the coil changes, time varying magnetic fields are generated. The magnetic field at the center of a circular loop of wire with radius r can be derived from the Biot-Savart law [18] and it is given by

$$B = \frac{\mu_0 I}{2r}. \quad (2.1)$$

To have a larger field, the number of loops of the circular coil N can be increased and (2.1) becomes

$$B = N \frac{\mu_0 I}{2r}. \quad (2.2)$$

Through Faraday's law of electromagnetic induction, voltage is induced in the same coil in the case of self-inductance. The voltage is given as

$$V = -\frac{d\Phi}{dt}. \quad (2.3)$$

where the magnetic flux $\Phi = \mathbf{B} \cdot \mathbf{A}$, \mathbf{A} is the vector with magnitude being the area enclosed by the coil and the direction being perpendicular to the coil. The \mathbf{B} field is assumed to be parallel to \mathbf{A} .

The voltage induces current in the direction which causes the induced magnetic field to oppose the magnetic field that causes the voltage, according to Lenz's law. This phenomenon is illustrated in Figure 2-3 [19]. It is difficult to calculate precisely the magnetic field that the coil inductor produces, except for some canonical cases, so in this development the coil is assumed to produce uniform field, taking the value of the field at the center point, i.e., (2.2). The coil inductance can be defined in terms of the voltage generated. It is the ratio of the induced voltage to the rate of change in the current as given below

$$L = \frac{V}{(dI/dt)} \quad (2.4)$$

On the other hand, the self-inductance of a coil is fundamentally defined as the flux linkage per unit current in the coil, stated as

$$L = \frac{\Lambda}{I} = \frac{N\Phi}{I} \quad (2.5)$$

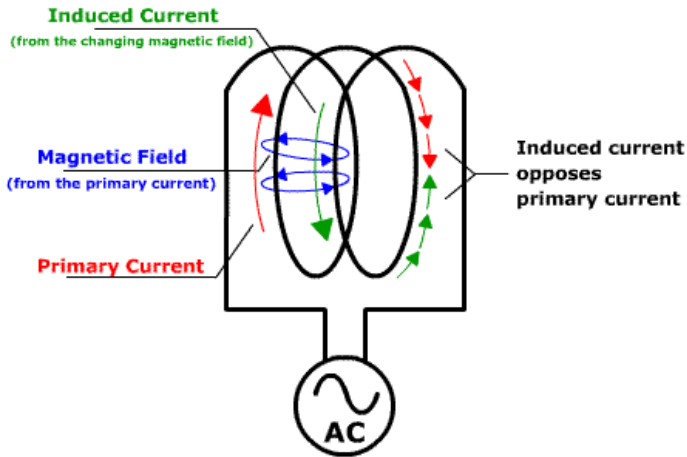


Figure 2-3: Electromagnetic induction in the coil [19]

2.3. Equivalent Model of the Coil

The transmitter coil can be represented by the equivalent circuit as given in Figure 2-4. Besides its inductive reactance, it has a resistance arising from the finite conductivity of the wire that it is made from. The coil resistance depends on the conductivity of the material used as well as the length of the coil wire and the wire cross section [20]. Consequently, the coil can be considered to be a perfect inductor connected to a resistor in series.

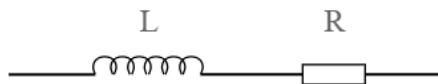


Figure 2-4: Coil Equivalent Model[20]

The equivalent series resistance introduces performance limitations to WPT systems as it causes resistive losses in the coil. Furthermore, when FOs are introduced to the coil, the interactions between the coil and the FOs can also be modeled with a perfect inductor and an equivalent series resistance. For example, eddy currents (induced currents in the FOs) causes the inductance to decrease and the coil resistance to increase. The phenomenon of eddy currents will be explained in Section 2.5.

2.4. Q factor

The quality factor commonly represented by Q is defined as the ratio of the maximum rate at which energy is stored in a circuit to the average rate of energy dissipation in the circuit.

The observed Q factor of the coil is a parameter at a specific operating frequency described as the ratio of the coil reactance to its resistance[21]

$$Q = \frac{\omega L}{R}. \quad (2.6)$$

It is dependent upon the frequency of the current flowing through the coil and therefore it will change according to the frequency of operation.

2.5. Eddy currents

When there is a changing magnetic field in a conductor, currents are induced within the conductor according to Faraday's law of induction. The flow of these currents is in closed loops within conductors in planes that are perpendicular to the magnetic fields that cause them. These loops of currents are generally referred to as eddy currents, like the currents seen on the water surface when paddling [22].

Factors affecting the magnitude of these eddy currents include

- magnetic field strength
- area of the current loops
- how fast or slowly the flux changes
- inverse proportionality to the resistivity of the conductor.

2.5.1. Power Loss

When the material is homogeneous, the time-varying magnetic field is uniform (at a given time) and skin effect is neglected, the power dissipated by eddy currents is given below from Bertotti's formula for power loss [22]

$$P = \frac{\pi^2 B_p^2 d^2 f^2}{6\rho D} . \quad (2.7)$$

where P is the power that is lost per unit mass (W/kg), B_p is the maximum magnetic field (T), f is the frequency of the current (Hz), d is the thickness of the sheet (m), ρ is the resistivity of the material ($\Omega\cdot\text{m}$) and D is the density of the material (kg/m^3).

At higher frequencies when the magnetic fields are changing very fast, they do not penetrate completely into the interior of the material (skin effect). The depth of the penetration of the magnetic fields in the conductor is then given by

$$\delta = \frac{1}{\sqrt{\pi f \mu \sigma}} . \quad (2.8)$$

where δ is called the skin depth of the material (m), distance beyond which the magnetic fields are attenuated significantly (i.e., cannot penetrate). μ is the permeability of the material (H/m) and σ is the electrical conductivity of the material (S/m). Power loss becomes independent of the skin depth when the metal thickness is bigger than the skin depth.

2.6. Magnetic properties of materials

Materials that are said to be magnetizable can have the magnetic moment of each atom of the material made to favor one direction. This can occur to different extents, which is referred to as the magnetization of the material. Since magnetic moment is a vector quantity with both direction and magnitude, magnetic moments of atoms in most materials may not be simply brought into alignment in one direction. The magnetic moments may cancel each other leading to weak magnetization [23].

All materials have a behavior where the atoms/molecules of the materials acquire an induced magnetic moment when subjected to a magnetic field. Electrons in orbital planes perpendicular to the incident magnetic field will slightly change their momentum. From Faraday's law, this change will cause the electrons to experience a force. Individual magnetic moments will no

longer cancel each other completely as these atoms/molecules acquire an induced magnetic moment.

When the induced magnetic moment is opposite to the applied magnetic field, the material is diamagnetic. Diamagnetic materials have only paired electrons. They are repelled by a nearby magnet, although the effect is extremely weak. All matter essentially have this diamagnetic property, although usually very weak[23]. In this project, samples tested that are diamagnetic are copper and zinc. On the other hand, paramagnetic materials have unpaired electrons and their magnetic moment is in parallel to the applied magnetic field hence making it stronger. They are attracted to a nearby magnet but still this attraction is weak as they can be knocked out of alignment with the magnetic field by thermal vibration. Paramagnetic materials have a permanent magnetic moment and have more powerful influence when an external field is applied. Paramagnetic materials tested in this research are aluminum and tin.

In the case of ferromagnetic materials, neighboring atomic magnetic moments have the tendency to become locked in parallel with their neighbors, exhibiting very strong interactions. The parallel alignment of moments results in large net magnetization even in the absence of a magnetic field. Ferromagnetic materials considered in this research include iron and nickel. Many alloys of these ferromagnetic elements also exhibit ferromagnetic behavior, and, in this research, stainless steel exhibited ferromagnetic behavior.

2.6.1. Permeability

Different materials get magnetized to different extents when a magnetic field is applied. The extent to which a material can gather magnetic flux is the permeability of the material. Materials with higher permeability are easily magnetized as the conduction of magnetic flux through the material is better. It is denoted by μ and defined by the ratio of the density of the flux to the magnetizing force[23], as given by

$$\mu = \frac{B}{H} . \quad (2.9)$$

Ferromagnetic materials have much higher permeabilities than non-ferromagnetic materials. Relative permeability, μ_r , of a material is more useful in this research as it shows more clearly how the presence of a material affects relationship between flux density and field strength by relating the quantity to the permeability of vacuum. It is the ratio of a material's absolute permeability to that of free space (vacuum) μ_0 [23], as given by

$$\mu_r = \frac{\mu}{\mu_0}. \quad (2.10)$$

Chapter

3. Methodology

There were two methodologies used in this research project. One was the experimental approach and the other was the simulation approach. The first method involved experimental measurements performed on the transmitter coil with the metal plates to accurately measure the inductance, equivalent series resistance and observed Q factor. The second method was a simulation of the physical set up in the electromagnetic software Ansys Maxwell for a few interesting cases to verify the validity of the experimental measurements.

3.1. Choice of Samples

To quantify the impact of surrounding objects, materials relevant to WPT systems had to be selected first. The first consideration in the selection process was to pick only materials that interact with electromagnetic fields and thus influence the magnetic and electric parameters of the coil. The second aspect in the consideration was to focus on materials that are mostly used in the manufacture of common foreign objects such as coins, keys and safety pins. These considerations mean that metals are of the most interest in this project. The data collected on the impact of different metals on WPT coil parameters would then provide a reference point to analyze the impact of various objects that contain these metals. Moreover, it was important to also consider the general systematic representation of the results to have a comprehensive database of predictions to be drawn from the samples.

3.1.1. Parameters of Interest

From their atomic structure and properties, metals are the most interactive and influential materials to an inductive WPT system. This is attributed to the fact that they are very good conductors of electricity and heat as they have free electrons moving in their lattices. Furthermore, they have permeabilities large enough to alter the permeability of the magnetic circuit of the coil. Pure metals behave differently when compared to their alloys. For this reason, several common alloys of pure metals were also considered. Further, most common objects consist also of a mixture of different metal types. However, for the alloys, those consisting of a principal metal (>50%) were of the most interest. This meant that most of the alloys considered contained a large percentage of a metal of interest alloyed with some other minor percentages of other metals.

To classify the metals, two parameters were considered, i.e., resistivity/ conductivity and relative permeability.

Resistivity/Conductivity

The conductivity of a material is the inverse of its resistivity. The two inversely related quantities can be used interchangeably, depending on the application. Metals with high conductivity have low resistivity and metals with low conductivity have high resistivity. Table 3-1 gives the standard conductivities of metals relevant to this study. One criterion used for sample choice was to choose sample metals that cover both high and low conductivity values. This criterion was also used in the selection of alloys.

Table 3-1: Material properties[24]

Metal	Magnetic Characterization	Conductivity(S/m) × 10⁷	Relative Permeability
Copper	Diamagnetic	5.85	1
Aluminum	paramagnetic	3.54	1
Zinc	diamagnetic	1.68	1
Nickel	ferromagnetic	1.46	600
Iron	ferromagnetic	1.04	5000
Tin	paramagnetic	0.87	1
Alloys	Primary metal		
Brass	Copper/Zinc	1.50	1
Bronze	Copper	0.60	1
Stainless Steel ¹	Iron	0.74	> 1

¹The exact relative permeability of the stainless steel used in this project is unknown. Different types of stainless steels give very different values, however, they tend to be ferromagnetic, with common values ranging from 40 to over 1000.

Relative Permeability

As stated in Section 2.6.1, the relative permeability (μ_r) is the ratio of the absolute permeability of a material (μ) to that of free space (μ_0). This value is 1 for most nonmagnetic materials but can have as high values as tens of thousands for more magnetic metals such as ferromagnetic metals. Table 3-1 gives the standard relative permeability values of the chosen metals. Those with relative permeability values of 1 or very close to 1 will henceforth be called non-ferromagnetic metals, whereas those with values substantially greater than 1 will be called ferromagnetic metals.

3.1.2. Metal Plate Size

Surrounding objects to an inductive WPT system consist of different sizes. Therefore, it is important to study the impact of metal plate size on coil parameters, especially in relation to the size of the transmitter used in this investigation. The outer coil diameter is 4.3 cm and is denoted by a . The inner diameter is 2.2 cm and is denoted by b as shown in Figure 3-1.

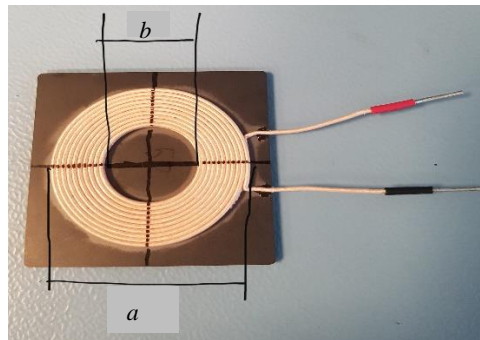


Figure 3-1: Coil with inner and outer diameter

The first consideration of plate size was to have an “infinitely large” plate that covers the entire coil and connecting terminals to encompass the entirety of the coil surrounding. For this case, the appropriate size (or plate area) was decided to be $15 \times 15 \text{ cm}^2$, which is 3.5 times the outer diameter of the coil or $3.5a$ in reference to the outer coil diameter of a . This would cover areas around the coil where the magnetic field is strong, as well as areas where it has become weaker and divergent. The next size of square metal plate was

selected to cover just the coil diameter a (i.e., 4.3 cm) to investigate the effects of reduced plate area on the magnetic field induced. Therefore, a $4.3 \times 4.3 \text{ cm}^2$ piece of metal was chosen. It covered areas of the coil where it was assumed that the magnetic field would be more concentrated. Thereafter, it was of interest to study the effect from a much smaller plate, corresponding to the coil inner diameter b (2.2 cm). This size was $2.2 \times 2.2 \text{ cm}^2$. The three chosen metal plate sizes are illustrated in Figure 3-2.



Figure 3-2: Metal plate sizes used in the study

3.2. Measurements

An LCR meter capable of taking measurements over a wide frequency range was used. The measurements were carried out over the wide frequency range of 1 kHz to 1 MHz (with 10 kHz resolution, except for the first two points of 1 kHz and 10 kHz). This range of frequency was practically significant because the frequencies used in the current Q_i standard lie within this range.

3.2.1. Experiment Setup

The experimental setup is depicted in Figure 3-3. The LCR meter used was Gw Instek LCR-8101G. It can measure over the range of frequencies from 20 Hz to 10 MHz. It has six-digit measurement resolution and the voltage can be driven up to 2 V. This meter has the measurement accuracy of 0.1%.

The LCR meter was connected to the ferrite-backed coil by two wires, and the metal plate was placed 2mm above the upper surface of the coil. 2 mm is the separation distance from the coil to the interface surface of the charging pad in normal Qi based transmitters for power profile below 5W. The readings from the LCR meter were transferred to a PC.

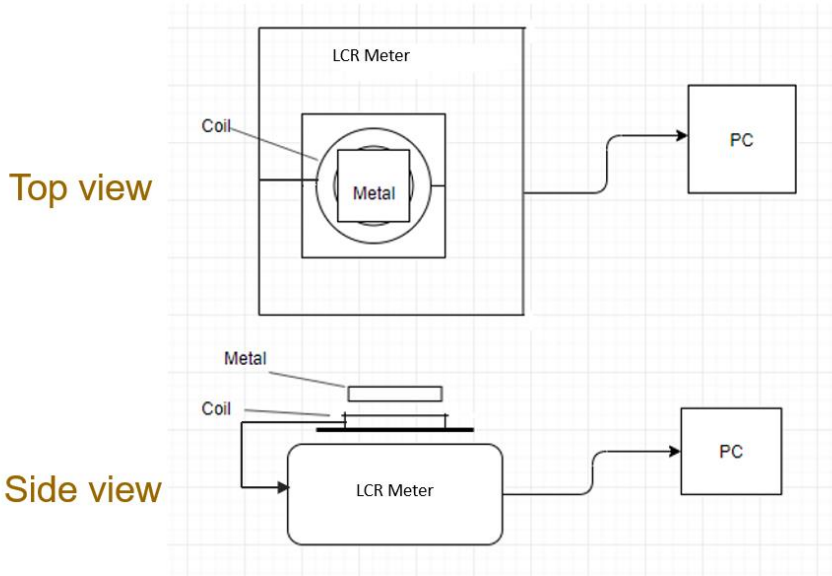


Figure 3-3: Experimental setup with the LCR meter, the coil with the square metal plate on top, and a PC for acquiring the measured data

3.2.2. Variables

The measurements were performed over frequency for several variables of interest, as explained below.

Size of Metal Plate

To investigate the impact of different metal plate sizes, three sizes were considered, as mentioned in Section 3.1.2. The first measurements were conducted with the $15 \times 15 \text{ cm}^2$ plates covering the whole area of the coil. Thereafter, $4.3 \times 4.3 \text{ cm}^2$ plates were investigated when placed on top of the metal to cover just the coil turns. The last size investigated was $2.2 \times 2.2 \text{ cm}^2$, where the plates covered only the inner coil diameter and left most of the coil turns uncovered. Further, interesting cases encountered, other sizes were also

considered, including $12 \times 12 \text{ cm}^2$, $10 \times 10 \text{ cm}^2$, $8 \times 8 \text{ cm}^2$, $6 \times 6 \text{ cm}^2$, $3 \times 3 \text{ cm}^2$, $2 \times 2 \text{ cm}^2$ and $1 \times 1 \text{ cm}^2$. This was an attempt to find an explanation on unexpected and not so obvious observed effects on coil parameters. Two cases in point were stainless steel and brass, to investigate the impact of plate size on equivalent coil resistance.

Thickness of Metal Plate

Thin metal sheet samples that were already available at nok9 were tested first. Initial measurements were performed on metal sheets that were less than 1 mm in thickness, specifically 0.05 mm. However, for the specific case of iron plates, three different thicknesses were tested: 1 mm, 2 mm and 3 mm. This was to verify an assumption from the analysis of the Bertotti's power loss formula that if the metal is thicker than the skin depth then the thickness of the metal does not influence the power loss from the eddy currents generated in the metal. In particular, a change in power loss is reflected in a change in the measured equivalent coil resistance.

Position of Metal Plate

This variable was relevant when it came to measure the smallest plate size considered, which was $2.2 \times 2.2 \text{ cm}^2$. The position of the plate on top of the coil was shifted around the coil to emulate the random positioning of a surrounding object on the transmitter coil.

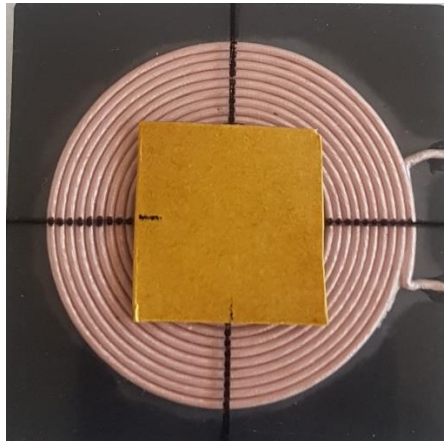


Figure 3-4: Metal plate position 1

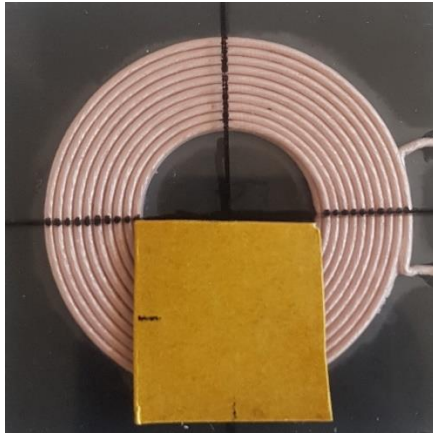


Figure 3-5: Metal plate position 2

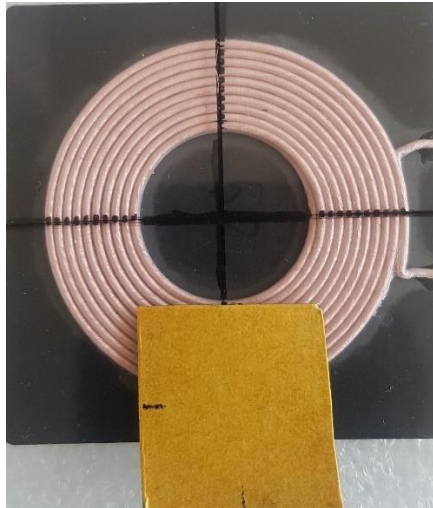


Figure 3-6: Metal plate position 3

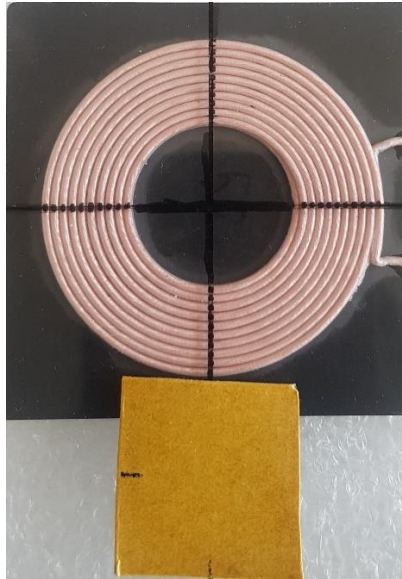


Figure 3-7: Metal plate position 4

3.3. Simulation

There are several low-frequency electromagnetic software that are popular in industry and academia. These include CST EM STUDIO[®], COMSOL Multiphysics and Ansys Maxwell[®]. Ansys Maxwell was chosen as the simulation package to validate specific experimental measurements.

Ansys Maxwell is a high-performance interactive software that uses finite element analysis to solve electric, magnetostatics, eddy current and transient problems[25]. It has several solution types, among which the eddy current solver was chosen. This solver can solve for sinusoidally varying magnetic field and impedances caused by alternating currents, as well as oscillating external magnetic fields. As implied by its name, there is also consideration for skin and proximity effects.

3.3.1. Simulation Model

The transmitter coil with its ferrite plate were modelled in Ansys, as given in the Figure 3-8. For getting the base structure, the program has predefined primitive base structures that one can configure to suit their desired model structure. Among the structures that the user could define, the polygon helix

user defined primitive was chosen as the base structure for the coil. It was configured to conform to the physical coil dimensions as given in Table 2-1.

Since the physical coil has two layers of ten turns, there was the need to have two layers of the coil connected. Further, the helix direction was swapped for one of the two coil layers (as for the physical coil), to have the currents in both layers flowing in the correct direction of reinforcing the field (instead of cancelling each other out).

Moreover, due to the high and exhaustive system memory usage that the program requires, the mesh was modified to be able to have faster run times. Electromagnetics structures are not as sensitive to mesh quality as for example mechanical and fluid mechanics models. Therefore, this was leveraged to have a mesh of a coarser size for faster run times and less memory requirement.

Further, in Ansys Maxwell, it is possible to have initial setup settings that do not need to be redefined every time the model is changed. One can also plot and view other variables once the set-up solution has been solved. This is beneficial for examining variables that had not been added to the solution set up before running the simulation. More information on Ansys Maxwell is available in the “Getting Started Guides” or “Maxwell Help online”[26].

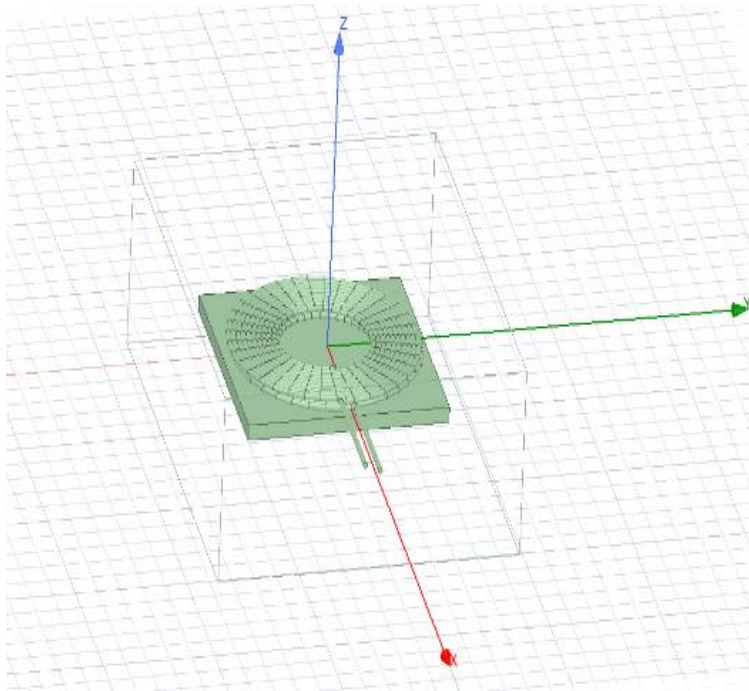


Figure 3-8: Ansys Maxwell model of the transmitter coil (backed by a ferrite plate) without a metal plate

3.3.2. Eddy Current Simulations

The first simulation model built was that of the transmitter coil (with a ferrite back plate) without any metal plate being placed above it. The physical characteristics of the coil were given in Section 2.2.

As the simulations were mainly intended for verification of the experimental measurements, only a few interesting cases were considered. However, there was a simulation-only study involving aluminum plate, where it was not possible to perform physical measurement due to unavailability of the desired metal thickness. Simulations were carried out mostly for sheets thinner than 1 mm since it was easier to source for thicker metal plates than thinner metal sheets for experimental measurements. Several simulated setups of the base model (coil without metal plate) together with the metal plate of the desired properties are elaborated below.

- a) $15 \times 15 \text{ cm}^2$ stainless steel metal plate of 0.05mm thickness

Stainless steel exhibited the most prominent and noticeable impact on coil parameters among the samples of metals tested. Therefore, it was considered in the simulation as a first verification of what was measured. This was done by simply adding the metal to the model given in Figure 3-8, with a separation distance of 2 mm as in the physical experimental set up. This is displayed in Figure 3-9.

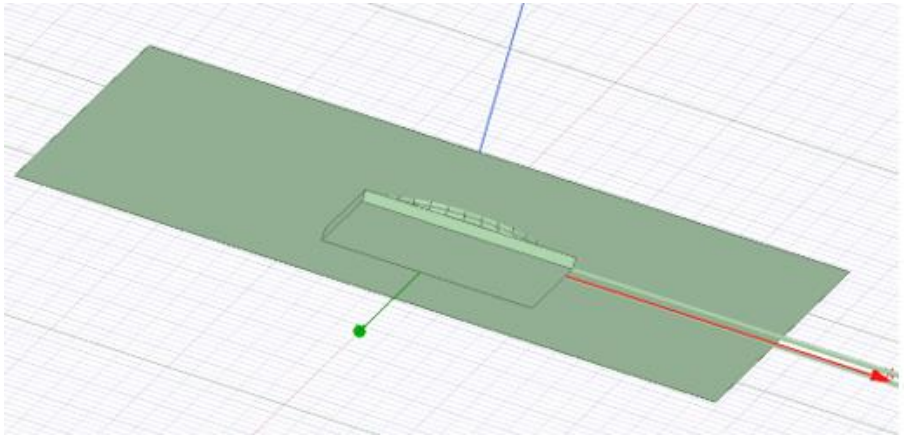


Figure 3-9: Coil with $15 \times 15 \text{ cm}^2$ stainless steel

- b) $2.2 \times 2.2 \text{ cm}^2$ stainless steel metal plate of 0.05 mm thickness placed in different positions above the coil

Experimental measurements of different positions of the $2.2 \times 2.2 \text{ cm}^2$ stainless steel sheet above the coil was another interesting case for verification in simulation. The metal positions as depicted in Section 3.2.2 were modelled as in Figure 3-10.

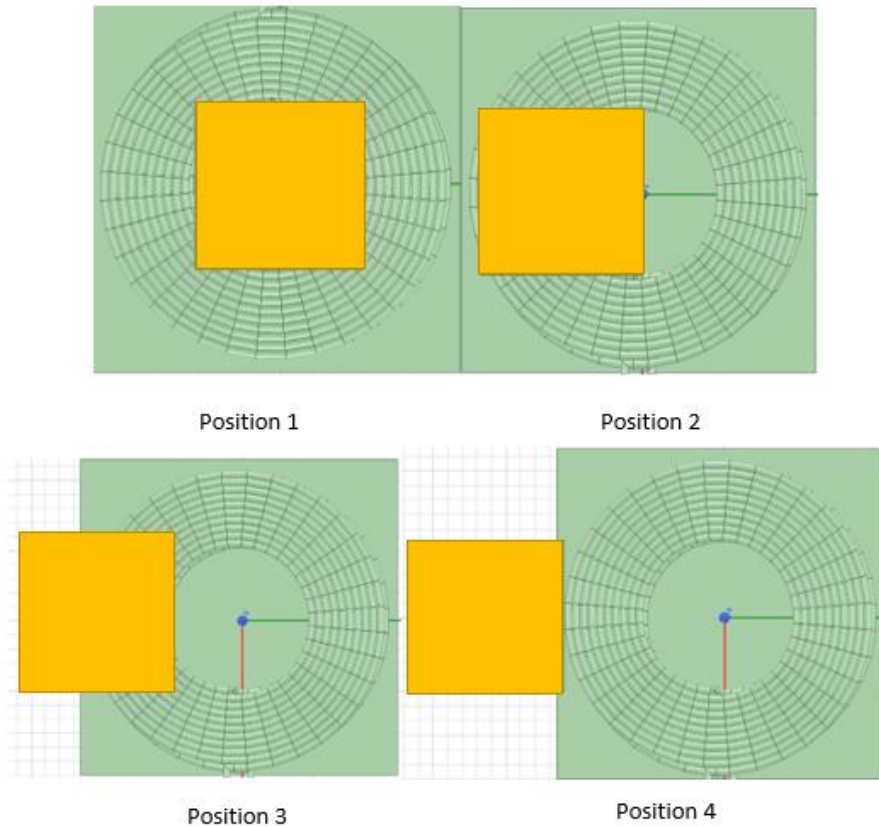


Figure 3-10: Coil with different positions of the $2 \times 2 \text{ cm}^2$ stainless steel plate above

c) *Different aluminum plate sizes*

Aluminum was an interesting metal for skin depth investigation since it has a relatively large skin depth for the frequency range under consideration. Aluminum skin depth ranges from approximately 2.6 mm at 1 kHz to $84 \mu\text{m}$ at 1 MHz. Since an aluminum sheet as thin as $16 \mu\text{m}$ could not be found for the measurement, the verification in simulation was done for this case for different plate sizes, without the metal thickness exceeding the skin depth for the frequency range of interest. Dimensions simulated were $15 \times 15 \text{ cm}^2$, $12 \times 12 \text{ cm}^2$, $10 \times 10 \text{ cm}^2$, $8 \times 8 \text{ cm}^2$, $6 \times 6 \text{ cm}^2$, $4.3 \times 4.3 \text{ cm}^2$, $3 \times 3 \text{ cm}^2$, $2 \times 2 \text{ cm}^2$ and

$1 \times 1 \text{ cm}^2$. Figure 3-11 shows an aluminum metal plate (or sheet) for one of the simulated sizes, i.e., $4.3 \times 4.3 \text{ cm}^2$.

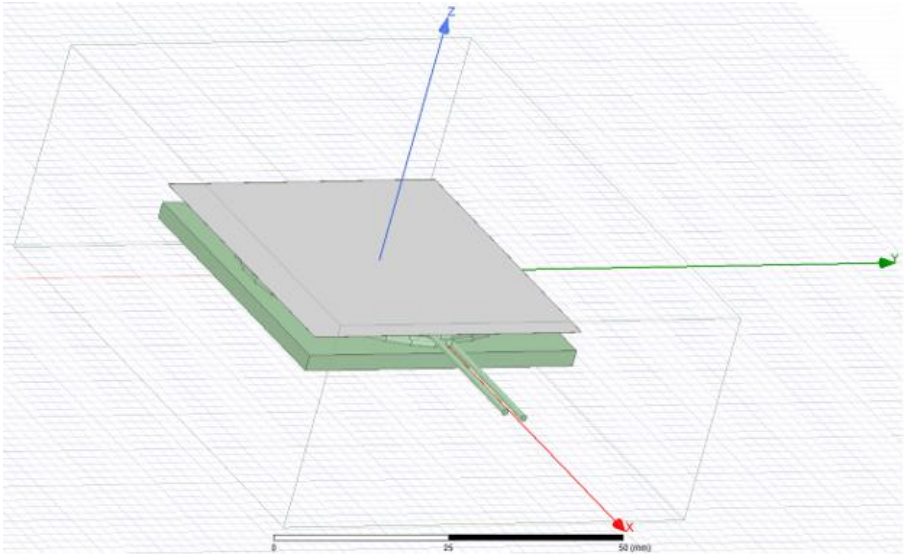


Figure 3-11: Coil with $4.3 \times 4.3 \text{ cm}^2$ aluminum plate 2 mm above

Chapter

4. Results and Analysis

This chapter gives the results that were obtained from experimental measurements and simulation. The first part gives the results from experimental measurements whereas the second part gives results from Ansys Maxwell simulations. Discussions are provided for the presented graphical results, together with possible reasons behind the results. The simulation part is intended for verifying experimental measurement as well as analyzing several interesting cases in more detail.

4.1. Experimental Measurements

Based on preliminary investigations of metal sheets already available at nok9 (brass, mild steel and stainless steel) and considering factors mentioned in Section 3.1.1, more metals were sourced and measured. Measurement results for the $15 \times 15 \text{ cm}^2$ metal plates are presented first. This metal plate size was considered as the base dimension (large enough to be considered an “infinite plate”). The effect of metal plate size was investigated by including in the experiments square metal plates of progressively smaller dimensions. The thickness of metals in this chapter is 1 mm unless stated otherwise. Metal thickness will be shown to have no significant difference in the impact on coil parameters if it is beyond skin depth of the metal. Results pertaining to varying the permeability and conductivity of the metal (by the choice of metal measured) are presented and discussed in terms of the general impact of these factors on coil parameters. Thereafter, results are given showing investigation of these variables: size, thickness and position of metal plate above the coil.

4.1.1. General Impact on Coil Parameters

Inductance

The coil inductance measured with no metal plate placed on top of the coil is approximately $24.5 \mu\text{H}$ and this will be the reference coil inductance value for later comparisons. As can be seen in Figure 4-1, this value remains relatively unchanged over the whole frequency range of measurement from 1 kHz to 1 MHz when there is no metal placed on top of the coil.

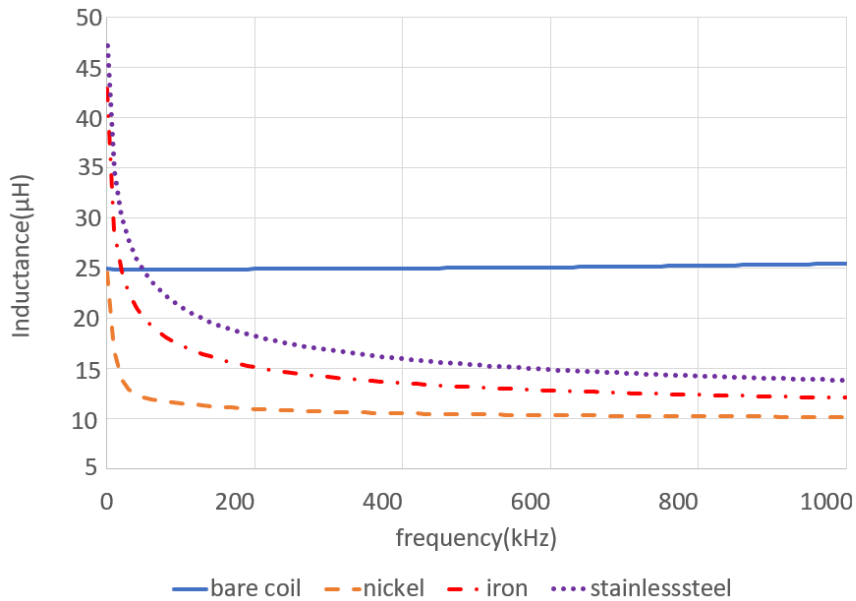


Figure 4-1: Coil inductance change with ferromagnetic metals

Ferromagnetic metals

Figure 4-1 shows the coil inductance as ferromagnetic metals (nickel, iron and stainless steel) were placed above the coil. When iron and stainless steel plates were placed on top of the coil, they caused the coil inductance to first increase above the reference value at frequencies below 50 kHz and then decrease below the reference value as the frequency increases beyond 50 kHz. Stainless steel caused the increase of up to around double the reference value (i.e., 47 μ H) whereas iron caused it to increase to 44 μ H. Iron crosses the reference value at approximately 20 kHz whereas stainless steel crosses the reference value at roughly 50 kHz. Nickel caused the coil inductance value to sharply decrease from the reference value for the range of frequencies of 1 kHz to 20 kHz. All three ferromagnetic metals caused the coil inductance to decrease below the reference value at frequencies beyond 100 kHz. The curve starts to flatten out at a much lower frequency for nickel than for iron and stainless-steel. However, the inductances of all three metals flatten out as the frequencies goes beyond 500 kHz.

The observed behavior can be explained as follows: At lower frequencies, the coil’s magnetic field magnetizes the metal, increasing the flux through the coil. Ferromagnetic metals having a higher permeability cause more flux to thread the coil, hence increasing the coil inductance more (e.g., iron has a

higher permeability than nickel, as seen in Table 3-1). As the frequency increases from zero (direct current or DC case), alternating magnetic field from the coil induces eddy currents in the metal, which produces an opposing magnetic field, thereby reducing the coil inductance. The magnetization effect (of increasing inductance) dominates at low frequencies whereas the effect from eddy currents (of reducing inductance) dominates at higher frequencies.

Non-ferromagnetic metals

The presence of non-ferromagnetic metals (copper, zinc, aluminum, tin, brass and bronze) caused the coil inductance to decrease below the reference value for the whole frequency range from 1 kHz to 1 MHz. In particular, the drop in the coil inductance occurred very rapidly as the frequency increases beyond 1 kHz, as can be seen in Figure 4-2 (focusing only on the range of 1 kHz to 60 kHz, since beyond 60 kHz, the values remain almost the same as those at 60 kHz). Copper caused the most reduction to the coil inductance relative to the reference value at 1 kHz, reducing it to below half of the reference value. Tin causes the least reduction to coil inductance in relation to the other non-ferromagnetic metals. However, for practical purposes, all these metals have almost the same coil inductance from 10 kHz onward, with only about 1 μ H variation among them.

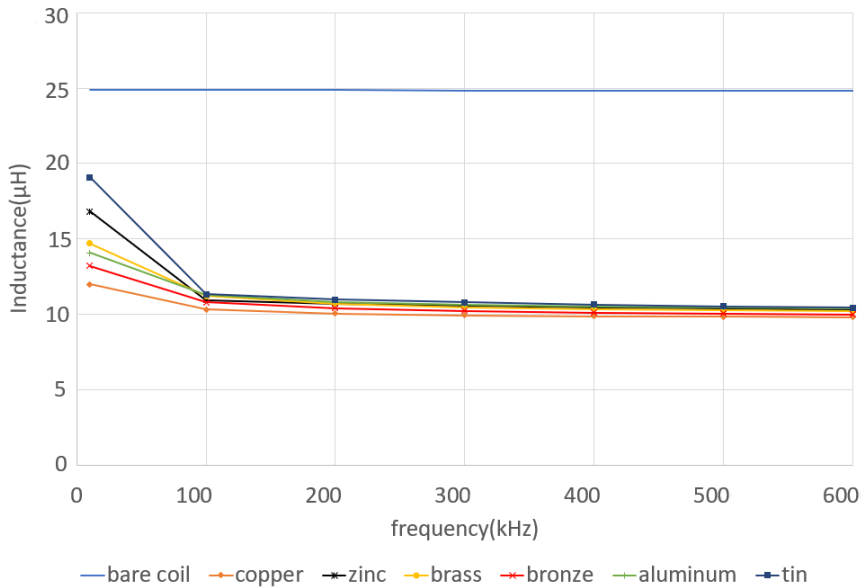


Figure 4-2: Coil inductance change with non-ferromagnetic metals

From the results, it is observed that metals with higher conductivity reduce the coil inductance more than metals with lower conductivity. For example, copper is more conductive than tin. One possible interpretation is that stronger eddy currents are induced in metals with higher conductivity. These currents cause a greater opposing magnetic field to the exciting magnetic field, which reduces the coil inductance more. The magnetization effect is almost non-existent for non-ferromagnetic metals, hence the coil inductance in the presence of these metals decreases below that of the reference value from DC onwards.

Resistance

The measured equivalent resistance of the coil without any metal plate placed on top of the coil shows a quadratic increase over the frequency range of 1 kHz to 1 MHz (due to skin effects in the coil conductor), with values increasing from 73 mΩ to 2 Ω. This is considered the reference case for the results on equivalent coil resistance, plotted in Figures 4-3 and 4-4.

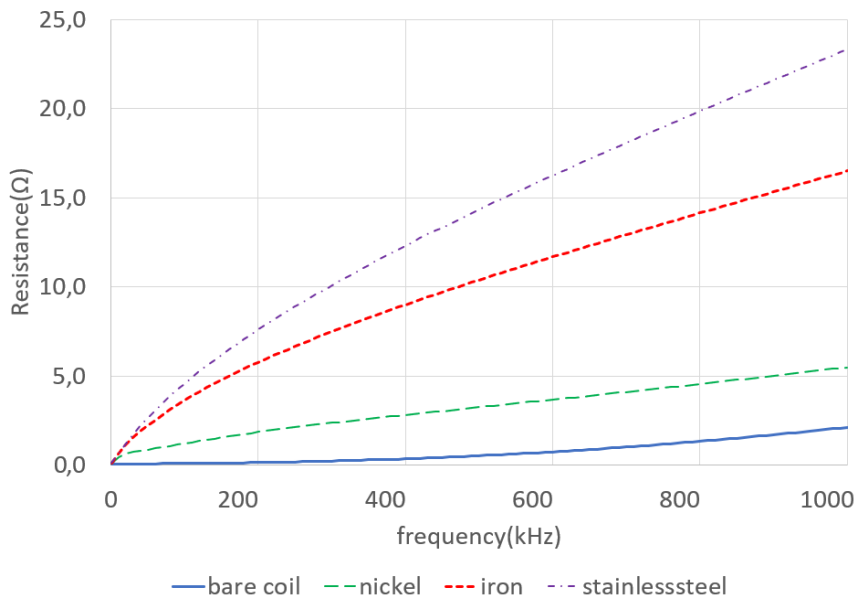


Figure 4-3: Equivalent coil resistance with ferromagnetic metals

The equivalent resistance of the coil in the presence of a metal plate increases above that of the reference case (of no plate) for all the metals. Stainless steel,

nickel and iron exhibit greater increases. Stainless steel and iron caused the effective resistance to increase to 23 Ω and 17 Ω , respectively, at 1 MHz. For non-ferromagnetic metals, tin caused the greatest increase to 2.6 Ω at 1 MHz.

This different impact on equivalent resistance can be explained by the generation of eddy currents in the metal. Eddy currents generated on the metal induce a magnetic field that opposes the driving current on the coil. Eddy current losses are reflected in the coil as losses from an additional resistor, which increases the effective resistance of the coil. A possible interpretation is that the metals that have lower conductivity have more resistance already in their structure and this is translating to the coil having a larger equivalent resistance. Metals with higher conductivity have less resistance, thereby causing a smaller increase in the equivalent resistance of the coil. For example, Table 3-1 shows that the conductivity of stainless steel is the lowest among the three ferromagnetic metals, whereas nickel has the highest conductivity, leading to the trend seen in Figure 4-3.

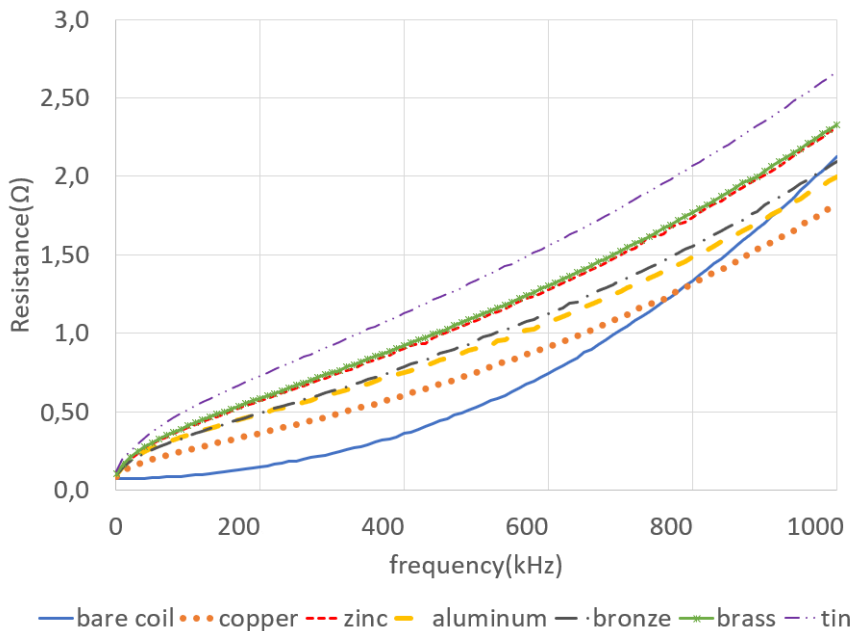


Figure 4-4: Equivalent coil resistance with non-ferromagnetic metals

Quality (or Q) factor

The quality factor for the coil, with ferromagnetic and non-ferromagnetic metal plates, is plotted in Figures 4-5 and 4.6. The Q factor of the reference case of the bare coil is also shown in both figures.

In all cases, the Q factor decreases when compared to the reference case. This is not surprising, since (2.6) shows that Q factor of the coil is the ratio of coil reactance (ωL) to coil resistance (R). In the case of ferromagnetic metals, the coil inductance ranges from about double the reference value to about half of the reference value. However, the equivalent coil resistance increases to more than double the reference values, hence the quality factor must decrease.

For non-ferromagnetic metals, the situation is simpler, in that coil inductance always decreased as compared to the reference case, whereas the coil equivalent resistance is almost always higher than the reference case (except for copper, bronze and aluminum above 800 kHz, where these cases present slightly lower coil resistance than the bare coil case). Therefore, the Q factor is also lower than the reference case for the non-ferromagnetic metals.

In addition, it can be seen that the Q factor is higher for non-ferromagnetic metals than for the ferromagnetic metals, mainly due to the smaller resistance seen by the coil in Figure 4-4 for non-ferromagnetic metals, as compared to Figure 4-3 for ferromagnetic metals.

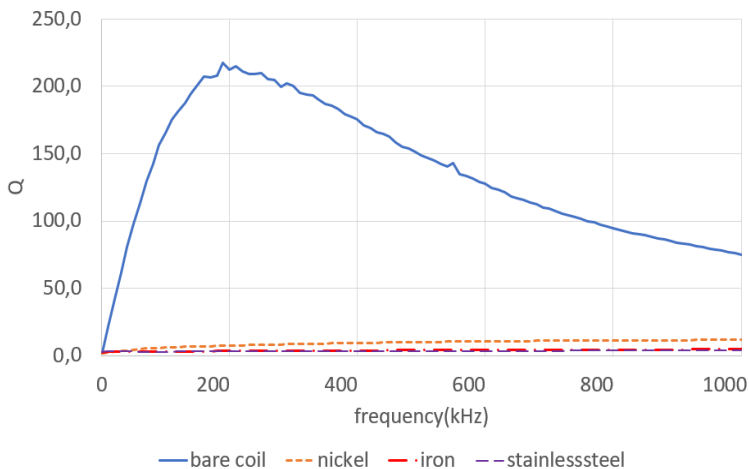


Figure 4-5: Observed Q factor with ferromagnetic metals

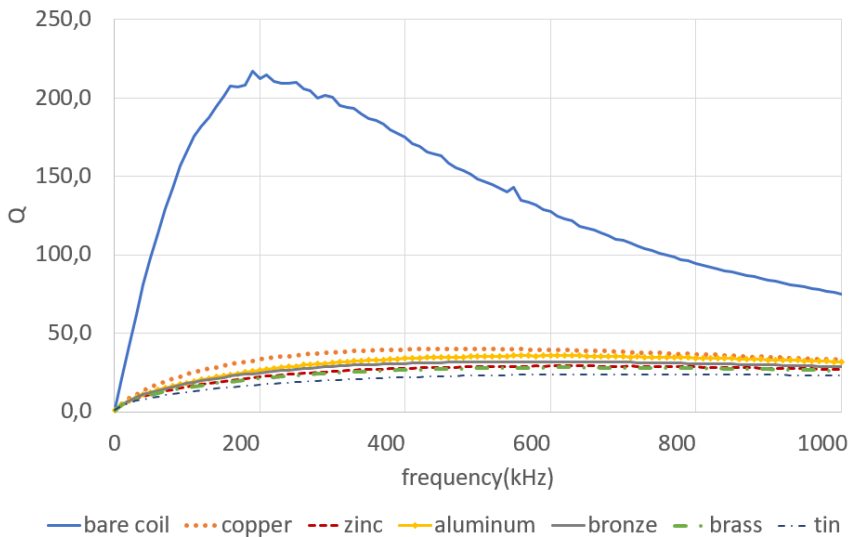


Figure 4-6: Observed Q factor with non-ferromagnetic metals

4.1.2. Impact of Different Sizes of Metal Plates

Measurements were performed to investigate the impact on coil parameters of different dimensions of the metal plates relative to the size of the coil. The first size was $15 \times 15 \text{ cm}^2$ as given in the preceding results. This was followed by measurements with $4.3 \times 4.3 \text{ cm}^2$ plates, the sides of which are equal to the outer coil diameter. The results are shown in Figures 4-7 and 4-8.

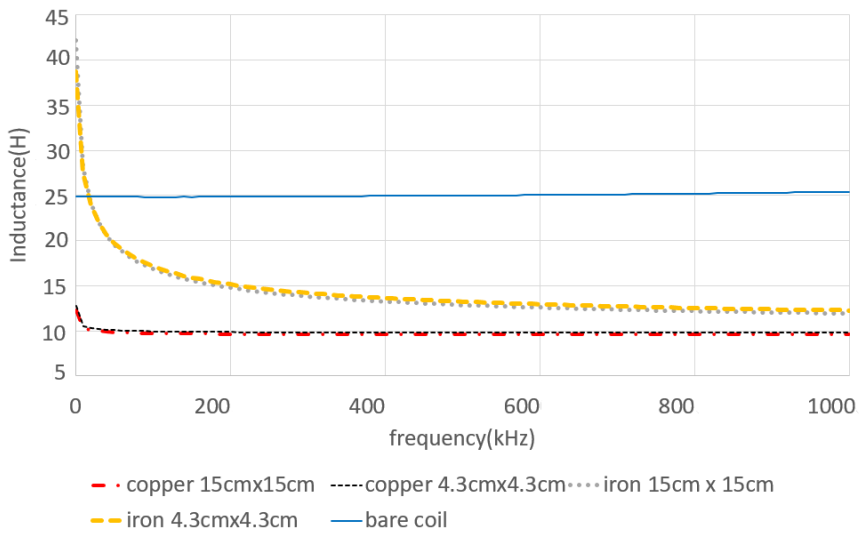


Figure 4-7: Size $15 \times 15 \text{ cm}^2$ and $4.3 \times 4.3 \text{ cm}^2$ plates on coil inductance

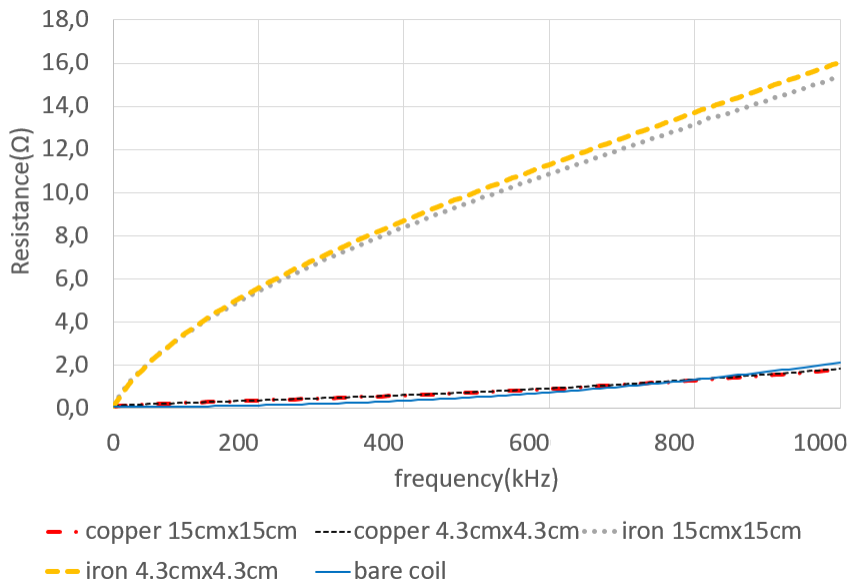


Figure 4-8: Size $15 \times 15 \text{ cm}^2$ and $4.3 \times 4.3 \text{ cm}^2$ plates on equivalent coil resistance

As can be seen in both figures, there is no significant difference in the coil parameters between the two metal plate sizes. $15 \times 15 \text{ cm}^2$ and $4.3 \times 4.3 \text{ cm}^2$

plates exhibit similar impact on the coil inductance. Equivalent coil resistance values for both dimensions are also similar to each other. Therefore, it can be concluded that, for both the ferromagnetic and non-ferromagnetic metals tested, metal plates of sizes beyond the size of the coil ($4.3 \times 4.3 \text{ cm}^2$) show no significant difference in how they impact coil inductance and equivalent coil resistance. This result indicates that the magnetic fields above the coil is well localized around the coil, such that different metal plate sizes do not matter, as long as it is larger than the coil size.

4.1.3. Impact of Different Thicknesses of Metal Plates

With the skin depth of metals tested calculated to be in the order of micrometers, measurements were performed to investigate the influence of metal thickness on coil parameters. Different metal thicknesses were tested: 1 mm, 2 mm and 3 mm. The results for one of the metals, iron, are given in Figure 4-9. The results show similar impact on coil inductance for three different thicknesses of the metal. This implies that the thickness of metal does not influence power loss from eddy currents generated in the metal, if the thickness of the metal is larger than the skin depth. This result makes sense, as the skin depth presents the depth to which the eddy currents are mostly confined.

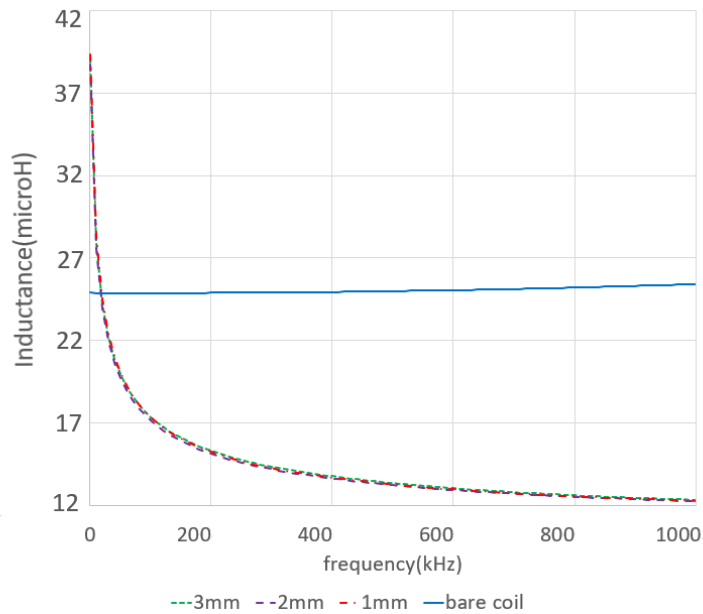


Figure 4-9: Iron plates of different thicknesses

4.1.4. Impact of Different Positions of Metal Plates

In this undertaking, the metal plate tested was a $2.2 \times 2.2 \text{ cm}^2$ stainless steel sheet of 0.05 mm thickness (i.e., thicker than skin depth). Stainless steel was chosen because it causes the largest impact on coil parameters (coil inductance and equivalent coil resistance) among the metals tested. The size of $2.2 \times 2.2 \text{ cm}^2$ is convenient to move into different positions around the coil. The results are given in Figure 4-10 for the impact on coil inductance and Figure 4-11 for the impact on equivalent coil resistance. There is more impact on the coil inductance when the metal plate is placed at the center of the coil. As can be seen from the graph, the impact on the inductance reduces when the metal plate is moved further and further away from the center of the coil.

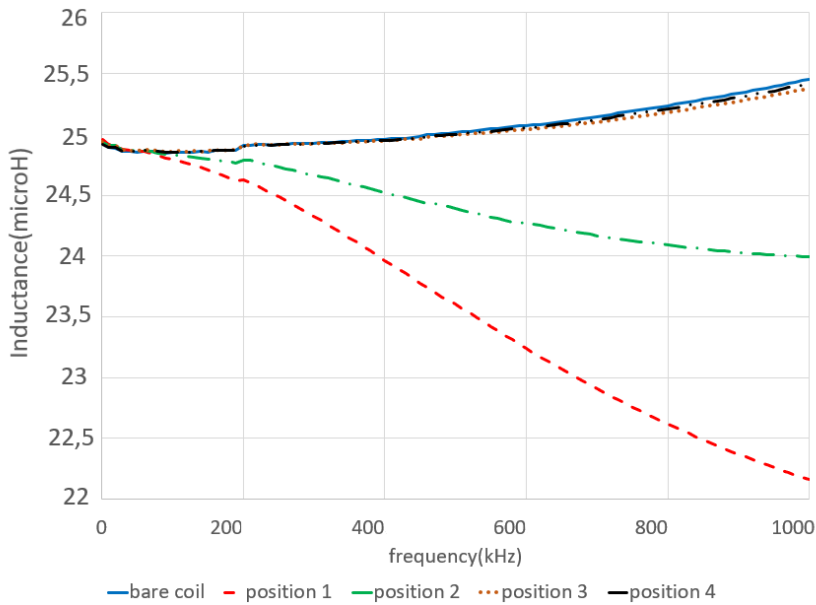


Figure 4-10: Coil inductance for different positions of metal plate

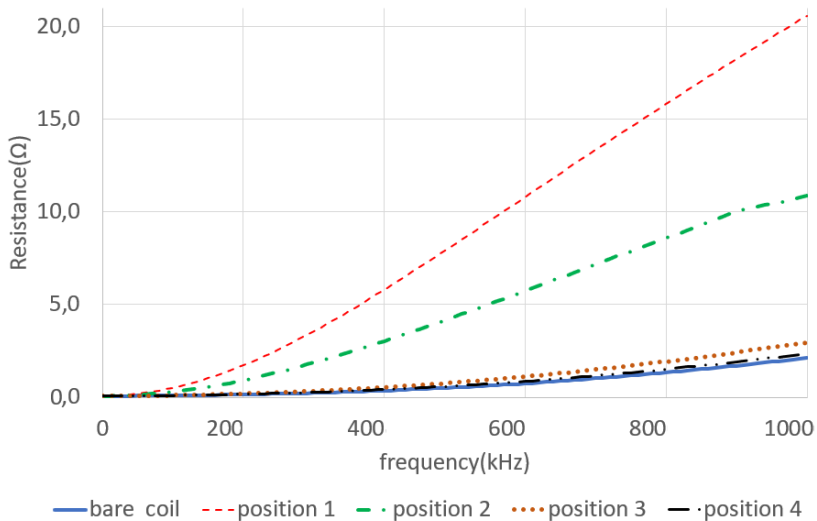


Figure 4-11: Equivalent coil resistance for different positions of metal plate

One possible explanation to this phenomenon is that the $2.2 \times 2.2 \text{ cm}^2$ plate at the center position covers the region of the coil that is assumed to have the

largest concentration of magnetic field (the center region without any wire). This in turn causes eddy currents to be induced in the metal, greatly reducing coil inductance. As the metal plate is moved away from this region of strong, uniform field, the weaker field impinging on the plate does not cause as much eddy currents to flow, causing less impact on coil inductance.

Similarly, it can be seen that positions with stronger eddy currents lead to higher equivalent coil resistance, therefore the same physics leads to position 1 having the highest equivalent coil resistance.

4.2. Ansys Simulations

Ansys Maxwell simulations were carried out for specific interesting cases for the validation of experimental results. Moreover, they were conducted to have a better understanding of results, through the visualization of current density distributions. The modelling of metal and coil is as described in Section 3.3.2.

4.2.1. Impact of Different Positions of Metal Plates

Experimental measurements performed to investigate the impact of metal plate position on coil parameters were modelled in Ansys and simulated. The case of $2.2 \times 2.2 \text{ cm}^2$ stainless steel plate was chosen, as stainless steel has the largest impact on coil parameters among the metals studied. Results from the simulation reveal close correlation to the experimental results, as shown in Figure 4-12 for equivalent coil resistance. Several possible reasons for the small differences between the simulation and experimental results include the limited accuracy in the mesh used in Ansys, imperfectly known material parameters, imperfect physical modelling of the object geometry and imperfect positioning of the metals. As mentioned before, Ansys is very computational resource intensive. To reduce run time, the mesh was reduced to a much coarser mesh than the recommended mesh. This will have affected the accuracy of the results. For the coil inductance, the simulation results lower than the measured results, again due to aforementioned sources of error in the simulation and experiments.

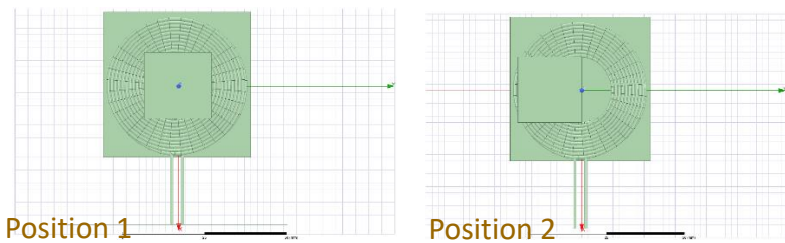
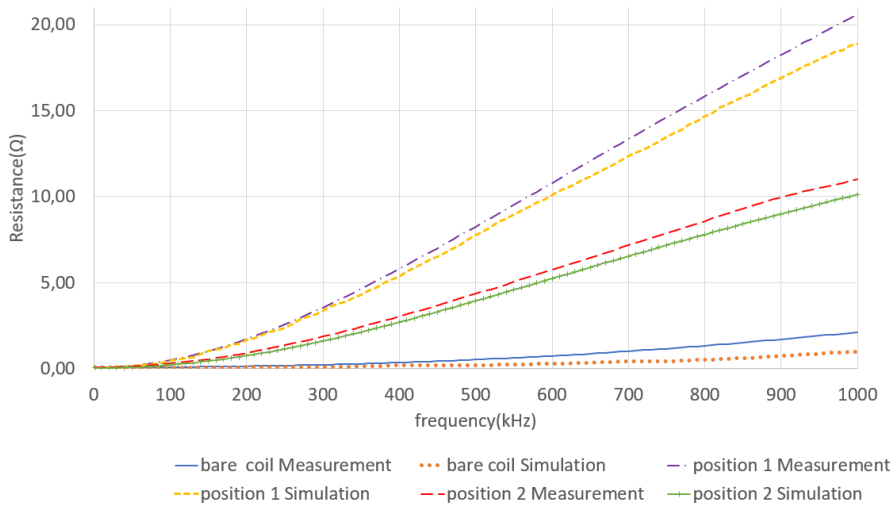


Figure 4-12: Ansys simulation effect on equivalent coil resistance with $2.2 \times 2.2 \text{ cm}^2$ stainless steel plate in positions 1 and 2

To gain more insight into the behavior of the currents for different metal plate positions, current density distributions from Ansys are plotted for positions 1 to 4 in Figures 4-13 to 4-16, respectively. As can be observed, the current density reduces as the metal plate is moved away from the center of the coil. There are more pockets of high current concentration (of eddy currents), when the metal is at the center of the coil. Some additional simulation results (not shown here) indicate that this is due to the strongest magnetic field penetrating the metal in this position. Moreover, the field is considerably weaker just above the wire loops, due to adjacent wires cancelling the field in between. It can be seen that the pockets of strong eddy currents are mostly confined to the inner or outer edges of the coil, where the magnetic field is the strongest.

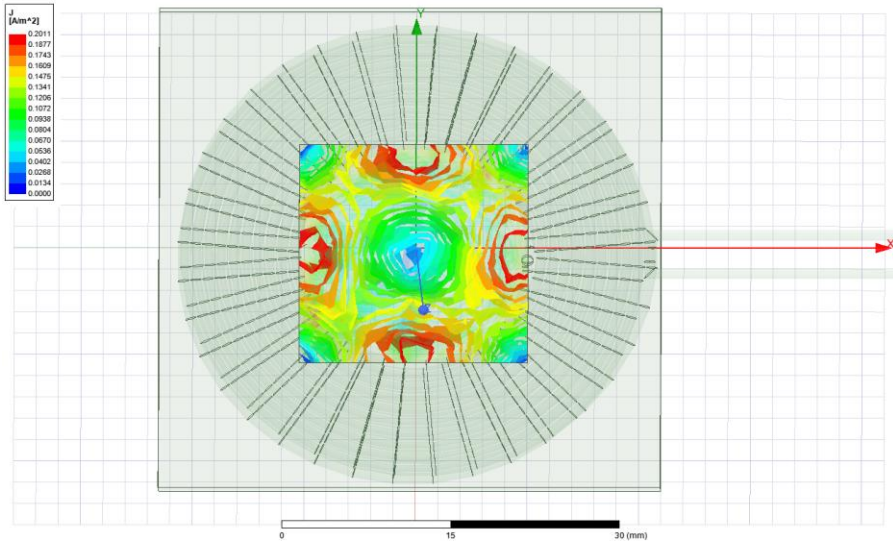


Figure 4-13: Current distribution for metal in position 1

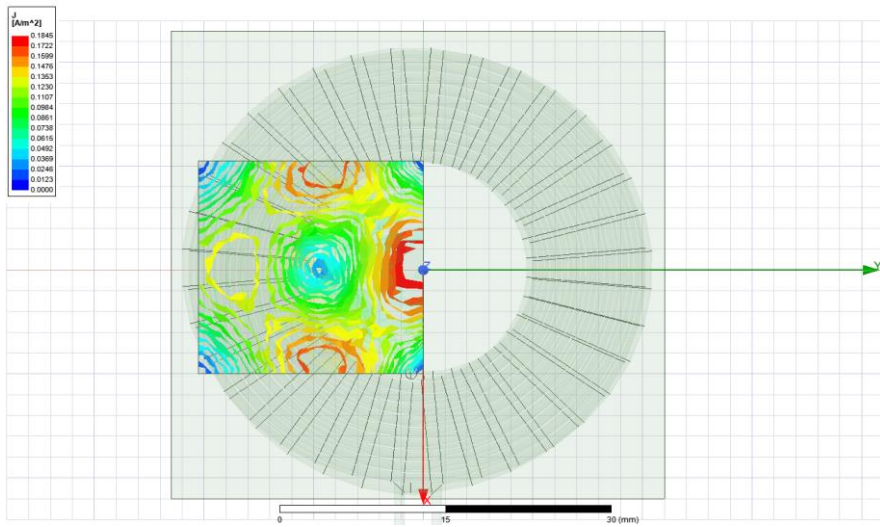


Figure 4-14: Current distribution for metal in position 2

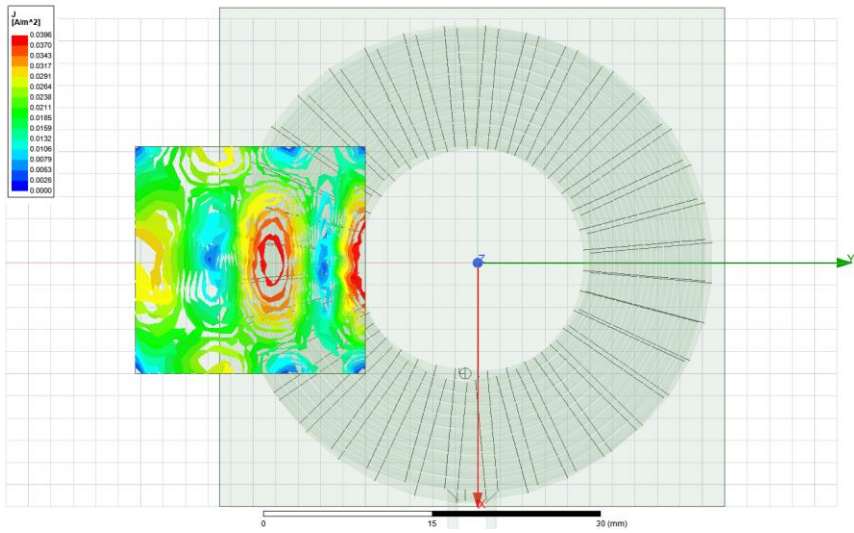


Figure 4-15: Current distribution for metal in position 3

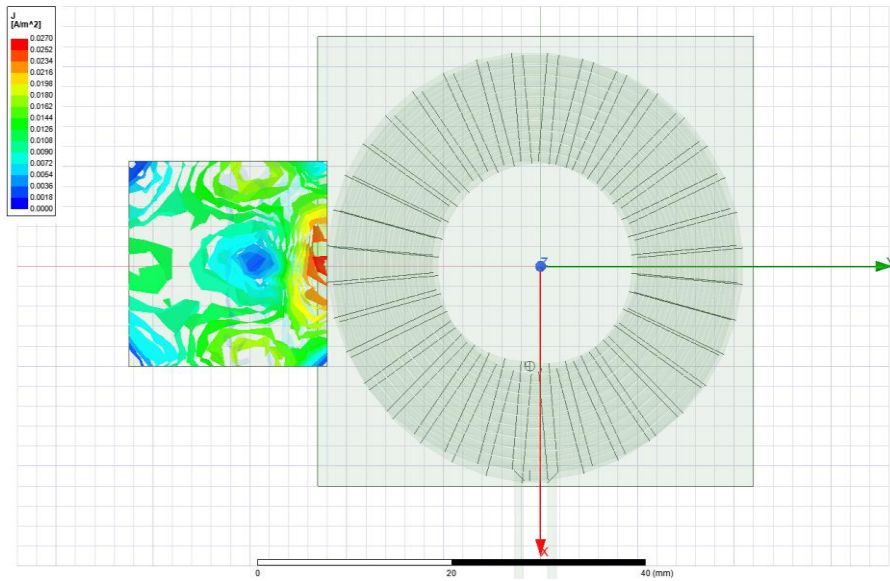


Figure 4-16: Current distribution for metal in position 4

4.2.2. Impact of Different Sizes of Aluminum Plates

Since aluminum has the largest skin depth among the chosen metal in the frequency range considered, it was interesting to investigate its effect on coil parameters for a thickness (i.e., $16\ \mu\text{m}$) smaller than the skin depth over the whole frequency range. This was modelled as described in Section 3.3.2. Results are given in Figures 4-17 and 4-18.

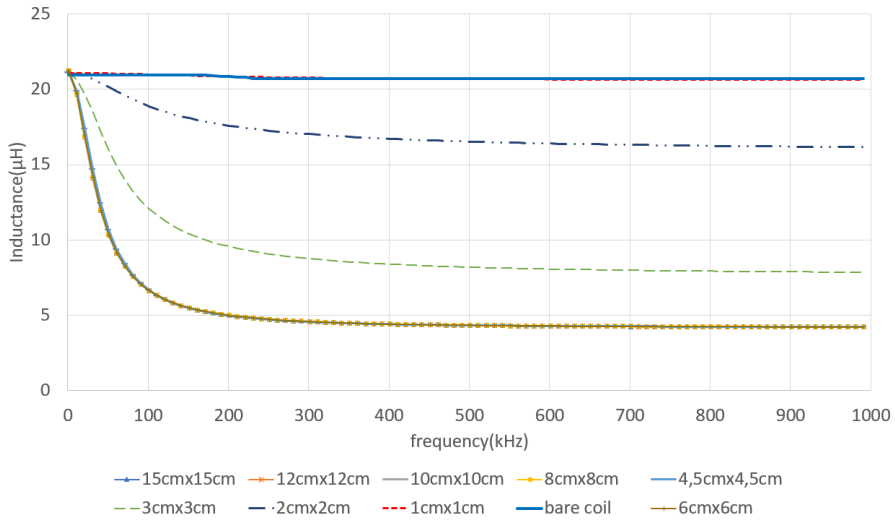


Figure 4-17: Ansys simulation of aluminum metal in different sizes effect on coil inductance

As can be seen in Figure 4-17, in general, larger plates cause the coil inductance to reduce more than smaller ones. However, beyond a certain size, the impact is unchanged (i.e., several curves overlapping). In Section 4.1.3, it was shown that metal sizes beyond the size of the coil exhibited similar impact on coil inductance. This behavior also occurs in the simulation with aluminum. Below $4.5 \times 4.5\ \text{cm}^2$, there is difference in impact on coil parameters for the different dimensions ($3 \times 3\ \text{cm}^2$, $2 \times 2\ \text{cm}^2$ and $1 \times 1\ \text{cm}^2$). However, from $4.5 \times 4.5\ \text{cm}^2$ and beyond, the size does not really change the impact on coil inductance.

The same general behavior is seen in the equivalent coil resistance. It is increased as the plate size increases from $1 \times 1\ \text{cm}^2$. With sizes beyond $4.5 \times 4.5\ \text{cm}^2$, there is no difference in the impact of the metal on the equivalent coil resistance. An explanation of this result is that for dimensions below the coil size, the eddy currents induced have less area to flow in and are weakened

by circulating on smaller arcs. Hence, they cause less induced opposing magnetic fields in the metal.

However, this explanation is not valid for the observation that the highest equivalent coil resistance values are obtained with the $3 \times 3 \text{ cm}^2$ aluminum plate, instead of the larger plate. This could be due to the wire-free area in the center of the coil having the strongest magnetic field, and the $3 \times 3 \text{ cm}^2$ plate capturing the strong field in the best manner (and not the field in the reverse direction, which may cancel the eddy currents induced by the strong field), since it is only slightly bigger than the wire-free region. Therefore, the eddy currents are strongest in this case, causing the most coil equivalent resistance to be produced.

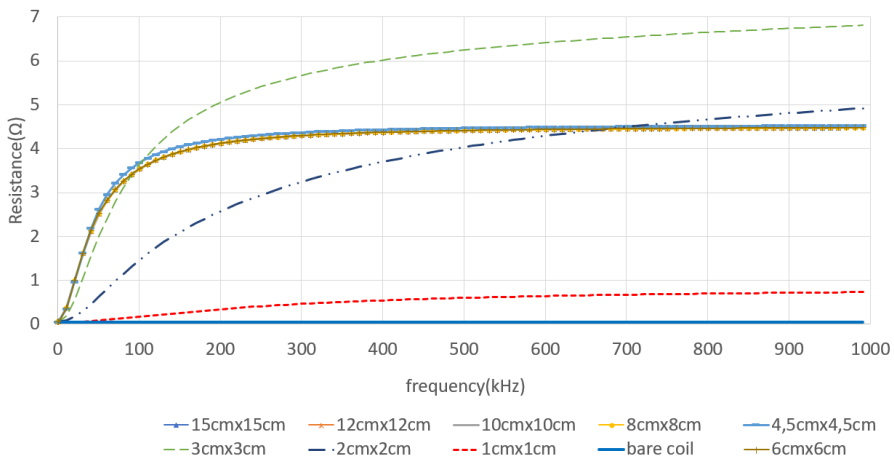


Figure 4-18: Ansys simulation of aluminum metal in different sizes effect on equivalent coil resistance

Chapter

5. Conclusions and Future Work

5.1. Conclusions

The thesis aims to quantify the effect of surrounding objects on coil parameters (mainly coil inductance and coil equivalent resistance), focusing on the cases of metal plates being above a coil.

For ferromagnetic metals, the magnetization effect, which causes coil inductance to increase beyond the reference value (of a bare coil), counteracts the eddy current effect, which decreases the coil inductance. However, the magnetization effect is expected to be largely frequency independent, whereas the eddy current effect becomes stronger as frequency increases (up to a certain frequency). For other metals, the magnetization effect is almost non-existent. Therefore, the coil inductance value would decrease below that of the reference value from DC onwards, since eddy current effects increase as the frequency increases. Each metal has a different characteristic frequency (knee point) at which the presence of the metal causes the coil inductance to remain at approximately the same value (i.e., converged). However, in all cases involving metal plates similar or bigger than the coil, the coil inductance values are largely confined between half to twice of the reference value, over the frequency range of 1 kHz to 1 MHz.

For the coil equivalent resistance, the presence of metals causes the resistance to increase. This is due to resistive loss from eddy currents, as can be expected. This increase in resistance is mainly responsible for the decrease in quality factor, particularly for ferromagnetic metals. Metals with higher conductivity are observed to cause lower resistance, resulting from lesser resistive loss in the metal plates. Further, resistive losses from eddy currents are independent of metal thickness when the thickness of the metal exceeds its skin depth.

The Ansys simulations performed to validate the experimental results produced results that show good correlation to the experimental results. Moreover, the simulations provided useful insights into the behavior of the coil parameters for selective cases of interest, including the impact of small metal plate position on coil parameters and the impact of different plate sizes. These results can be explained using the current density and magnetic field

distributions provided by the simulation tool. In particular, the eddy current distributions on the metal plate largely determine the resulting impact on the coil parameters.

5.2. Future Work

To extend this work, it will be interesting to investigate the impact of metal plates for the scenarios presented in this thesis, when a receiver coil is included in the setup. This will facilitate a study into how the metal object influences the coupling factor and mutual inductance of the coil system, when it is subjected to the conditions presented.

Another area of interest for future work is to examine the sources of error between measurement and simulation results in more detail. By improving the agreement of these results, the simulation tool can be used more effectively and reliably to study the effect of surrounding objects on coil parameters, including cases which may be theoretically interesting but difficult to implement in practice.

References

- [1] R. Kumar and P. Padalkar, "Wireless Charging Market," Allied Market Research, 2018.
- [2] G. Bekaroo and A. Seeam, "Improving Wireless Charging Energy Efficiency of Mobile Phones: Analysis of Key Practises," in IEEE International Conference on Emerging Technologies and Innovative Business Practices for the Transformation of Societies (EmergiTech), Bonne Terre, MO, 2016.
- [3] A. Tomar and G. Sunil, "Wireless Power Transmission: Applications and Components," International Journal of Engineering Research & Technology (IJERT), vol. 1, no. 5, pp. 1-8, 2012.
- [4] International Telecommunication Union "Applications of Wireless Power Transmission via Radio frequency beam," Report ITU-R SM.2392-0, Geneva, Switzerland, 2016.
- [5] "Wireless Power Consortium," [Online]. Available: <https://www.wirelesspowerconsortium.com/about/about-wpc>. [Accessed: 1 May 2019].
- [6] N. Tesla, "The True Wireless," The Electrical Experimenter, May 1919.
- [7] J. Garnica, R. A. Chinga, and J. Lin, "Wireless Power Transmission: From Far Field to Near Field," Proceedings of the IEEE, vol. 101, no. 6, pp. 1321-1331, 2013.
- [8] A. M. Jawad, N. Rosdiadee, S. K. Gharghan, H. M. Jawad, and M. Ismail, "Opportunities and Challenges for Near-Field Wireless Power Transfer: A review," Energies, vol. 10, no. 1022, pp. 1-28, 2017.
- [9] V. Muratov, "Methods of Foreign Object Detection in Inductive Wireless Charging," [Online]. Available: <https://www.wirelesspowerconsortium.com/data/downloadables/1/9/0/9/wpc1704-vladimir-muratov-methods-for-foreign-object-detection.pdf>. [Accessed: 2 June 2019].
- [10] L. Lan, N. M. Ting, S. Aldhafer, G. Kkelis, C. H. Kwan, J. M. Arteaga, D. C. Yates, and P. D. Mitcheson, "Foreign Object Detection for Wireless Power Transfer," in 2nd URSI AT-RASC, Gran Canaria, Spain, 2018.

- [11] N. Kuyvenhoven, C. Dean, J. Melton, and A. Umenei, "Development of a Foreign Object Detection and Analysis Method for Wireless Power Systems," in 2011 IEEE Symposium on Product Compliance Engineering Proceedings (ISPCE), San Diego, CA, 2011.
- [12] J. Pávó, Z. Badics, S. Bilicz, and S. Gyimóthy, "Efficient Perturbation Method for Computing Two-Port Parameter Changes Due to Foreign Objects for WPT Systems," IEEE Transactions on Magnetics, vol. 54, no. 3, pp. 1-4, 2018.
- [13] W. Xiao, R. Shen, B. Zhang, D. Qiu, Y. Chen and T. Li, "Effect of Foreign Metal Object on Soft-Switching Conditions of Class-E Inverter in WPT," Energies, vol. 11, no. 1926, pp. 1-19, 2018.
- [14] M. N. O. Sadiku, Elements of Electromagnetics, Oxford: Oxford University Press, 2010.
- [15] "murata Innovator in Electronics," [Online]. Available: <https://www.murata.com/en-global/products/emiconfun/emc/2015/05/26/20150526-p1>. [Accessed: 1 June 2019].
- [16] "The Qi Wireless Power Transfer System Power Class 0 Specification," Wireless Power Consortium, 2018.
- [17] L. Swaans, "Requirements Specification on TPT#MP1 coil assembly," Technical Doc. no. MR-RS-17-0013, nok9 AB, Malmö, Sweden, 2017.
- [18] OpenStaxCollege, "Magnetic Fields Produced by Currents: Ampere's Law," [Online]. Available: <https://opentextbc.ca/physicstestbook2/chapter/magnetic-fields-produced-by-currents-amperes-law/#import-auto-id1166991829247>. [Accessed 4 April 2019].
- [19] B. Crouse, "Self-Inductance and Inductive Reactance," NDT Resource Center, 4 March 2002. [Online]. Available: <https://www.nde-ed.org/EducationResources/CommunityCollege/EddyCurrents/Physics/selfinductance.htm>. [Accessed: 4 April 2019].
- [20] A. Ahmed, "Equivalent Circuit Diagram for a Coil," Iamtechnical, 2017. [Online]. Available: <http://www.iamtechnical.com/equivalent-circuit-diagram-coil>. [Accessed: 18 May 2019].
- [21] J. Bird, Electrical Circuit Theory and Technology, Oxford: Newnes, 2003.
- [22] J. Henry, "Eddy Currents," Princeton University, [Online]. Available: http://www.princeton.edu/ssp/joseph-henry-project/eddy-currents/eddy_wiki.pdf. [Accessed: 12 February 2019].

- [23] R. Clarke, "Magnetic Properties of Materials," University of Surrey, 2 August 2008. [Online]. Available: <http://info.ee.surrey.ac.uk/Workshop/advice/coils/mu/#mu>. [Accessed: 13 December 2018].
- [24] "Tibtech Innovations," [Online]. Available: https://www.tibtech.com/conductivite.php?lang=en_US. [Accessed: 5 June 2019].
- [25] Ansys, "Maxwell 3D User's Guide," Ansys Inc., Canornsburg, 2012.
- [26] "Ansys Maxwell," [Online]. Available: <https://www.ansys.com/products/electronics/ansys-maxwell>. [Accessed: 3 March 2019].